Preliminary Investigations on Monitoring the Snow Water Equivalent Using Synthetic Aperture Radar

R. LECONTE
Canada Centre for Remote Sensing
1547 Merivale Road
Ottawa, Ontario K1A 0Y7, Canada

T. CARROLL
National Remote Sensing Hydrology Program
Office of Hydrology
National Weather Service, NOAA
6301 34th Avenue South
Minneapolis, Minnesota 554050, U.S.A.

P. TANG
Saint John River Forecast Centre
Department of the Environment
P.O. Box 6000
Fredericton, New Brunswick E3B 5H1, Canada

ABSTRACT

A research project was undertaken to evaluate the utility of airborne Synthetic Aperture Radar (SAR) data for the estimation of SWE over open areas. This cooperative effort involved the cooperation of the Canada Centre for Remote Sensing, the St. John River Forecast Centre, and the U.S. National Weather Service. In addition to the SAR acquisition, the study involved extensive ground measurements in the region of Woodstock and Perth-Andover, New Brunswick. Preliminary results suggest that SAR data may be suitable for the extraction of SWE values over open areas. Future effort will focus on a thorough quantitative analysis of the data, in which the effects of topography, surface roughness, vegetation, and the snowpack structure on the ability to extract SWE values will be evaluated.

INTRODUCTION

Snow is a major component of the hydrological cycle in temperate and boreal environments. As such, snow cover properties, such as the snow water equivalent (SWE) and the areal extent of the snowpack, have been identified as among the most important parameters for flood forecasting, hydroelectric reservoir management, and in water supply and demand management across most of North America. Unfortunately, traditional measurement techniques (snow courses) may not provide accurate and frequent estimates of SWE and snow areal extent over moderate to large areas. Improved water balance estimates could be achieved by increasing the number of snow courses, however, this would result in increasing costs and sampling time. Remote sensing offers new possibilities to snow hydrology because large areas can be quickly investigated at minimum costs. Unfortunately, the presence of clouds can severely compromise the efficiency and limit the potential usefulness of the "traditional" optical sensors (such as Landsat and SPOT) for snow cover monitoring. Microwave systems, on the other hand, are virtually weather independent, which gives them a significant advantage over optical systems for obtaining repeated coverage of a given area.

This paper will describe a cooperative project initiated by the Canada Centre for Remote Sensing (CCRS) in conjunction with the St. John River Forecast Centre (RFC) and the US National Weather Service (NWS), for the estimation of SWE in open areas using active microwave methods. Airborne Synthetic Aperture Radar (SAR) data were collected over a portion of the St. John River Basin during the 1989-1990 winter season. The airborne data collection program was supported by an extensive ground truth program (snow courses) and airborne gamma ray surveys of SWE.

MICROWAVES AND SNOW

Microwaves occupy the portion of the electromagnetic spectrum between 0.3 and 300 GHz (100 and 0.1 cm). However, frequencies employed in remote sensing typically fall within a much smaller window, 1 to 37 GHz (30 to 0.8 cm). Microwaves in this window travel almost unimpeded through the atmosphere, which confers to systems operating at those frequencies the ability to penetrate through clouds.

Snow is a three-component mixture consisting of air, ice particles, and liquid water. At temperatures below 0^0C, snow is said to be dry, since it contains no "free" liquid water. It will, however, contain small amounts of "liquid-like" water in thin films around, and bound to, ice crystals (Hobbs, 1974).

The air and ice that constitute dry snow have different electrical properties, which is reflected in the value of their dielectric constant. The microwave response properties of snow-covered terrain depend strongly, among other factors, on the dielectric properties of the snow volume. The combination of air (dielectric constant $\epsilon = 1$) and ice ($\epsilon = 3.2$) results in dry snow having a ϵ between 1.2 to 2.0 for snow densities ranging from 0.1 to 0.5 g/cm3 (Hallikainen and Ulaby, 1986). In wet snow, however, the high value of the dielectric constant of liquid water (typically around 80 at frequencies of 1 to 10 GHz) is such that, even with small amounts of free water in a snow pack, the resulting dielectric constant is substantially increased.

Two factors give dry snow a unique behaviour with respect to microwaves. First, microwave energy can penetrate the pack without being significantly absorbed (Matzler and Schanda, 1984). The dry snow is said to be "lossless". The second factor is that, because the microwaves can enter the snow volume, they can be subjected to scattering within the pack. It is the combination of these properties which confers to the microwaves the potential for remote sensing SWE.

Liquid water in the snow presents two complications for microwave remote sensing (Bernier, 1987). First, small amounts of liquid water in a snow pack turns the snow into a "lossy" medium. The wet snow will absorb most of the microwave energy, with little scattering occurring. Because the penetration depth of the pack (depth to which 63% of the microwave energy is absorbed) is reduced to the order of one wavelength with a 4-5% snow wetness (Matzler and Schanda, 1984), scattering is limited to a thin layer and retrieval of SWE becomes impractical. The second problem relates to the difficulty of measuring the snow liquid water content in the field (Colbeck, 1978), especially at shallow depths where complete penetration of the microwaves through the pack may occur.

The present study focuses on interactions of dry snow with microwaves in the 3.1 - 5.7 cm wavelengths (9.8 to 5.3 GHz).

ACTIVE MICROWAVE SYSTEMS FOR SWE ESTIMATION

Techniques for microwave remote sensing can be classified as either passive or active. Passive systems employ downward pointing radiometers which record natural upwelling microwave energy. Such radiometers have been aboard many satellites, and their potential for measuring SWE has been demonstrated by various researchers (Goodison, 1989; Rango et al., 1989; Chang et al., 1987). The ground resolution of these systems is on the order of 30-50 km.

Active systems, such as SAR, emit microwaves toward the ground and measure the reflected, or backscattered, signal. The SAR is an imaging system, in that it converts the backscattered energy into digital values that can be displayed as video image. It is also a side-looking system, meaning that the microwave beam is emitted at an angle off the nadir flight line. SAR can achieve a much finer resolution than passive systems, typically in the order of 10-100 meters. To date, the only satellite which carried a SAR onboard was SEASAT, which was launched in 1978 and decommissioned after only three months because of a major electrical failure. Consequently, research in the use of active sensors for SWE extraction has been limited to a few ground-based scatterometer experiments (Stiles and Ulaby, 1980; Matzler and Schanda, 1984) and airborne missions (Goodison et al., 1980; Bernier and Fortin, 1989; Leconte and Pultz, 1990). Although encouraging results have been obtained, no algorithms have been developed for extracting SWE from SAR data. With the advent in the 1990's of many

SAR platforms (ERS-1 in 1991, RADARSAT in 1994, EOS dedicated platform in 1998-99) there is a need for increased research in this area.

The amount of backscatter received by the SAR antenna is the sum of surface scattering at the snow-air interface, volume scattering within the snowpack, scattering at the snow/soil interface and volumetric scattering from the soil. Atmospheric scattering is usually very small and can be neglected. Figure 1 illustrates the concept.

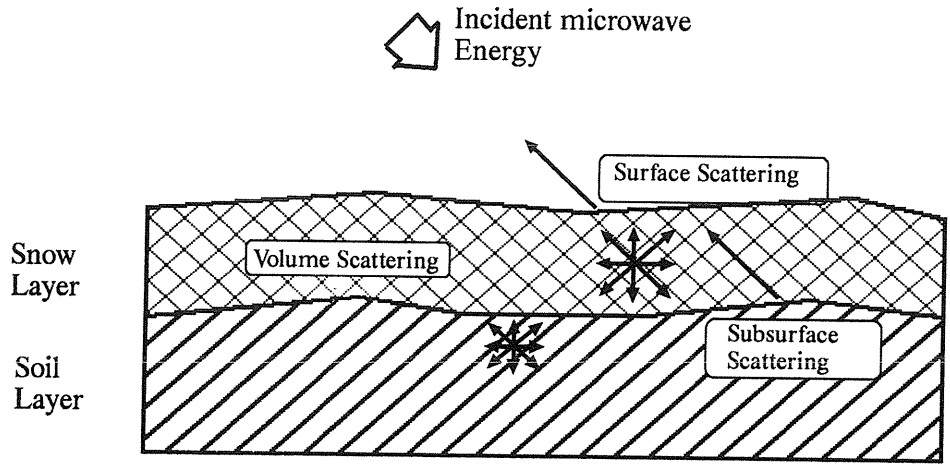

Figure 1: Scattering mechanisms in a snow covered surface

Volume scattering in dry snow is the result of dielectric discontinuities in the electric properties of ice crystal and air. The level of scattering is strongly influenced by scene and instrument parameters. Scene parameters include the structural properties of the pack (crystal size and shape, and stratigraphy), and the snow depth and density. Volumetric backscatter increases with an increase in snow quantity (Stiles and Ulaby, 1980). For a given wavelength, scattering increases with snow grain size and layering (Bernier, 1987). The most significant instrument parameter is probably the microwave wavelength. Typically, wavelengths shorter than snow crystal size (0.05 to 1 mm) are strongly scattered even by the thinnest snowpack, while wavelengths longer than 10 or 15 cm travel almost unaffected through most seasonal dry snowpacks (Bernier, 1987).

In addition to the snowpack characteristics, the soil surface roughness, soil moisture levels, and overlying vegetation are parameters whose influence on the total backscatter signal will be significant, especially at longer wavelengths. Schanda (1987) observed that at lower microwave frequencies (longer wavelengths) the measured backscatter values were strongly affected by reflections from the soil below the snow cover due to the large penetration depth in dry snow. Leconte and Pultz (1990) noted that, depending on the soil surface roughness, an increase in SWE could result in either an increase of the total backscatter signal (caused by an increased volumetric scattering), or a decrease of the total radar return (resulting from a reduced contribution from the soil surface caused by attenuation in the snowpack). This makes estimating SWE from SAR data a difficult task because of the problem in discriminating between volumetric scattering within the snowpack and surface scattering at the ground/snow boundary. The problem increases in complexity in a forested environment, as trees scatter most of the incident microwave energy, especially at shorter wavelengths, with little left energy reaching the snowpack. To date, research has been limited to open areas (Goodison et al., 1980; Bernier and Fortin, 1989; Leconte and Pultz, 1990).

Finally, when the snow is dry, the contribution from the air/snow surface is negligible because of the small dielectric discontinuity at the boundary, and can usually be neglected (Stiles and Ulaby, 1980).

SAINT JOHN RIVER BASIN STUDY

Study Site

The study site is located in the potato cultivation belt in western New Brunswick, north of Woodstock and south of Perth-Andover. The area extends 40 km E-W and 90 km N-S (Figure 2).

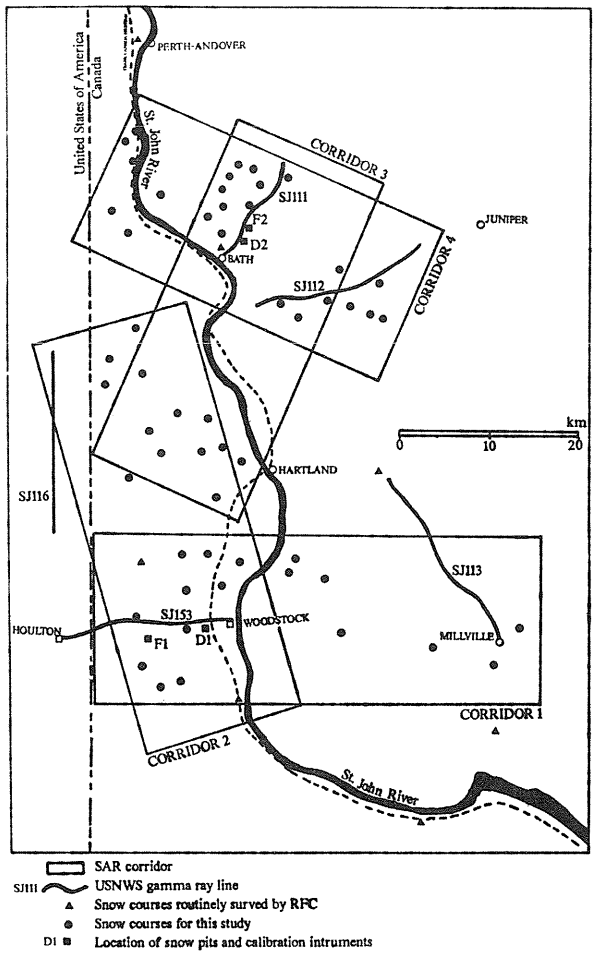

Figure 2: Study site

The St. John River runs through the study area in a N-S direction. The area west of the river is characterized by a rolling topography, where more than 30 percent of the surface area is agricultural land. Snow depth is relatively uniform over the region, with a small increase toward the north and west. Snow records indicate that SWE accumulation typically reaches 100 mm. The study area located east of the St. John River is characterized by rougher terrain, with elevations ranging from less than 100 meters at the river to more than 250 meters in the eastern most section. Accordingly, variations in SWE are more pronounced, with values typically between 100 and 175 mm. This area is mostly forested, with about 10-15 percent of land devoted to agriculture, mainly in the Bath area (see Figure 2). The St. John RFC routinely performs snow surveys at a few locations in or around the study area. Gamma ray surveys are also conducted once or twice a year by the NWS. The location of the snow survey courses and gamma ray flight lines is also shown in Figure 2.

SAR Experiments

The system used is the C/X SAR system installed in CCRS's Convair-580 aircraft. It is a digitally controlled, two-channel radar, operating simultaneously at C (5.7 cm, 5.3 GHz) and X band (3.2 cm, 9.6 GHz), transmitting microwave energy at either horizontal (H) or vertical (V) polarization and receiving both polarizations simultaneously. It was demonstrated that this system could discriminate targets with very low backscatter values, making it well adapted for monitoring SWE. Data can be acquired in three nominal imaging modes: "nadir", "narrow swath", and "wide swath". The characteristics of the imaging modes are described in Table 1. A more detailed description of the system can be found in Livingstone et al (1988) and will not be repeated here.

Table 1: Imaging modes of the C/X SAR system

Mode	Incidence angle (deg) from	to	Resolution (m) Range	Azimuth	Swath width (km)
Nadir	0	74	6	6	22
Narrow swath	45	76	6	6	18
Wide swath	45	85	20	10	63

Note: the specifications are for an optimum aircraft altitude of 6 km.

Two SAR flight missions took place during the 1989-1990 winter season. Ideally, the SAR flights were to occur so that temporal differences in SWE would be maximized. The target window for the first mission was from November 15 to December 15. The first SAR deployment occurred on December 13 and 14 1989, when the snow cover was relatively thin, although in some locations the SWE had already reached 70 to 80 mm. The second flight mission occurred on February 6 and 7 1990, one week following a storm that left approximately 45 cm of snow in the Fredericton area.

The corridors that were imaged cover a surface area of approximately 3000 sq. km (Figure 2). The study site is roughly subdivided into two sub-areas, the West site (west of the St. John River) and the East site. The West site is mostly covered by corridors 1 and 2 (see Figure 2), while corridors 3, 4, and a portion of corridor 1 cover the East site. The rationale for selecting two distinct sub-areas was based on the snow conditions usually encountered in those areas. Typically, the Woodstock site is characterized by relatively uniform snow depths and SWE, while a strong gradient in SWE is usually encountered at the East site due to variations in elevation.

On each mission, the four corridors were flown 2 to 4 times, covering various combinations of polarizations (HH, HV, VV) and incidence angle ranges (0-74 degrees for nadir mode; 45-76 degrees for narrow swath mode).

In order to extract quantitative information on geophysical parameters, such as SWE, SAR data need to be calibrated. This can be achieved by deploying, in the study area, point targets of known reflectance values (or "radar cross section" in the microwave jargon). The brightness of each pixel making a SAR image is then converted into a radar backscatter value (absolute calibration), or is adjusted to another SAR data set (relative calibration), with algorithms using radar cross section values and SAR system parameters as input data.

Point targets that were used for the SAR experiments are trihedral Corner Reflectors (CR) and Active Radar Calibrators (ARC). A trihedral CR consists of three metal plates assembled together to form orthogonal planes. The size and geometry of the reflector determines its radar cross section, which in turn is related to the brightness of the target on a radar image. A CR will appear as a single bright point on a SAR image. An ARC is an electronic device which receives the incident microwave signal, amplifies and modulates it, and returns a signal corresponding to a target of known cross section. A "recirculator" allows more than one bright point to appear on a radar image.

Snow Data Collection Campaign

Snow Surveys:

There were 52 open fields identified for the snow sampling exercise (Figure 2). In addition, 4 fields were selected for the deployment of the ARCs and CRs. Two sites were used for the December mission (D-1, D-2), and February mission (F-1, F-2) (Figure 2).

The selected fields covered surface areas ranging from 20 to 200 hectares, and the elevation varied from 100 to more than 300 meters. Some fields were sheltered by wood lots, while others were more exposed to wind. The intent was to select fields which would represent a wide range of SWE accumulation both spatially (from field to field) and temporally.

Coinciding with the mid-December flight, samples were taken at 50 sites for both snow depth and water equivalent. Depending on the variability of the measurements obtained, three to five snow samples were taken using a Mount Rose Federal snow sampler. The distance between the samples was approximately 30 meters.

On February 6 and 7, only 37 of 52 sites were sampled due to the shortage of personnel and unfavourable weather conditions. Estimates were made for the remaining 15 sites based on a partial survey carried out on March 2 along with local weather data. Results of the surveys are summarized in Table 2. Values of SWE were corrected to account for positive biases introduced by the sampler. A 10% overestimate in SWE was assumed (Goodison, 1978).

Table 2: Results of the snow surveys, December 89 and February 90

	West site (27 fields)		East site (25 fields)	
	Dec. 89	Feb. 90	Dec. 89	Feb. 90*
mean SWE (mm)	51	113	59	132
max SWE (mm)	107	176	87	190
min SWE (mm)	17	27	25	81
mean depth (cm)	31	44	32	51
max depth (cm)	49	76	45	83
min depth	13	18	18	28

* Values for 15 fields were estimated from a survey on March 2, 90.

The fields had also been visited before and after the snow season and the following information was collected:

- ground cover type (bare, vegetated);
- tillage practice (row direction, row spacing, peak-to-trough height);
- surface roughness (smooth, intermediate, rough, based on a visual interpretation of the surface).

The field characterization was supplemented by ground photographs. At least three shots were taken for each field: a vertical photograph showing fine scale details of the surface; an oblique photograph showing vegetation and tillage practice; and a photograph covering most of the field.

Airborne Gamma Radiation Snow Measurements:

The U.S. National Weather Service has developed and maintains the National Operational Hydrologic Remote Sensing Center based in Minneapolis, Minnesota. The Center is responsible for making airborne snow water equivalent measurements and satellite areal extent of snow cover measurements over the U.S. and southern Canada. The airborne and satellite snow cover data are provided in real-time and used operationally by various federal, state, provincial, and private agencies in the U.S. and Canada when issuing spring flood outlooks, water supply forecasts, and river and flood forecasts.

The technique used to make airborne snow water equivalent measurements uses the attenuation of natural terrestrial gamma radiation caused by the mass of the snow cover. Root mean square errors are typically less than 1.0 cm of snow water equivalent over agricultural environments and approximately 2.0 cm over forested areas. The technique requires the estimation of the background gamma radiation, which is a function of soil moisture and obtained by flying the area in absence of a snow cover. Details of this technique and the associated errors have been thoroughly discussed by Carroll and Carroll (1990, 1989A, 1989B) and by Glynn, et al. (1988) and will not be presented here.

Airborne data are routinely collected over the St. John River basin. Each flight line is typically 16 km long and 300 m wide covering an area of approximately 5 sq km. Consequently, each airborne snow water equivalent measurement is a mean areal measure integrated over the 5 sq km area of the flight line.

On February 7-12, 1990, an airborne gamma radiation snow survey was conducted over 49 previously established flight lines in the St. John River basin. One additional flight line (SJ153) was added to the operational network in support of this study. Consequently, no background radiation data for flight line SJ153 were available to directly calculate snow water equivalent using the appropriate background radiation measurements. Nonetheless, it is possible to estimate the background radiation for SJ153 from the mean of the background radiation data for three nearby flight lines and to infer a reasonable airborne snow water equivalent value for the line. The average background radiation, normalized to 25 percent soil moisture for lines SJ113, SJ116, and SJ117, were used to estimate the background radiation for SJ153.

Some estimate of mean soil moisture conditions in the upper 20 cm of soil is required to calculate snow water equivalent. Since no ground-based soil moisture data were available for this analysis, typical values ranging from 15-35 percent gravimetric soil moisture were used.

Table 3 presents the results of the February, 1990, survey for the five lines of specific interest to this study: SJ111, SJ112, SJ113, SJ116, and SJ153, and using gravimetric soil moisture estimates of 15, 25, and 35 percent. Overall, the airborne gamma SWE estimates were higher than the snow survey data. A possible explanation for this apparent discrepancy lies in the fact that only open fields were surveyed, as opposed to the 5 sq km coverages of the gamma ray lines, which included both forested and open sites. The closest fit was observed along the flight lines SJ111 and 112 with a 35% gravimetric soil moisture (respectively 133 and 151 mm as compared to average ground measurements of 130 and 153 mm), a mostly agricultural area.

Table 3: Results of the Gamma Ray survey, February 90

FLIGHT LINE	SOIL MOISTURE	SWE (cm)
SJ111	15	16.2
SJ112	15	18.1
SJ153	15	15.2
SJ111	25	14.7
SJ112	25	16.5
SJ113	25	16.0
SJ116	25	17.5
SJ153	25	13.7
SJ111	35	13.3
SJ112	35	15.1
SJ113	35	14.5
SJ116	35	16.0
SJ153	35	12.2

Snow Pit Measurements:

Coinciding with the SAR overflights, the snowpack was characterized from measurements obtained in snow pits. Jones (1983) recommended use of at least one snow pit for each SAR flight corridor. Due to limited resources, however, it was decided to minimize the number of snowpits by locating them at the intersections of flight corridors. These locations coincide with those of the calibration targets (Figure 2).

The variables and parameters measured in the snow pits were: snow depth, SWE, snow density using a Mount Rose snow sampling kit; vertical temperature profile using thermoresistors;

vertical density profile using a portable snow density kit; vertical dielectric profile using portable dielectric probes (Brunfeldt, 1987); crystal shape and size using a magnifying lens; and depth of layers in the snowpack.

The snowpack December 89 was observed to be homogeneous, that is there was no layering present. The density increased slightly with depth from approximately 0.15 to 0.20. SWE was found to be 64 mm and 38 mm at locations D-1 and D-2, respectively. Crystals had angular shapes and a diameter ranging from 0.5 to 1.5 mm. The snowpack was said to be dry during the SAR overpass. The measured temperature in the pack hence remained below 0^0C. Air temperature varied from -16 to -12^0C, and the first few centimeters of the ground were frozen.

During the February 1990 mission, the snowpack was more stratified, and the grains were more rounded and bonded (melt-freeze metamorphism) . The diameter of a typical cluster of grains averaged 2-3 mm. The SWE and snow density had increased significantly, with average values of 97 mm and 0.27 for site F-1, and 102 mm and 0.30 for site F-2. The temperature in the pack remained below 0^0C during the SAR flight, again preserving a dry pack. This was confirmed by dielectric measurements which never exceeded 2.05. The soil surface was frozen, and temperature measurements at the bottom of the snow pack were very near the freezing point (-1^0C at F-1, and -2^0C at F-2). This may suggest that, due to inherent variations in soil cover type, aspect, and SWE, the entire surface of some fields may have not been completely frozen. This was confirmed on a few occasions during the snow surveys.

Description of the Imagery

Although the primary objective of this study is to develop a methodology to extract quantitative information on the snowpack from SAR data, a qualitative analysis of the imagery is an essential first step. This type of analysis would provide insight on specific mechanisms and processes which should contribute to the radar backscatter as observed on the images. The quantitative analysis of the SAR data has only been recently initiated and no preliminary results are yet available. Due to space limitations, only the C-HH image of line 4 will be presented here.

December 89 Data:

The C-band HH nadir mode data of line 4 is shown in Figure 3. This image represents raw SAR data (no geometric or radiometric corrections) produced from the Real Time SAR Processor on board the aircraft. The look direction is south, meaning that the radar illumination is from north to south (top to bottom on the figure). The uneven illumination in the across track direction (perpendicular to the flight line) is the result of an unequal distribution of the microwave energy across the swath. Note the compression of the data in the top portion of the figure. This compression is an inherent characteristic of any imaging radar as radars are side looking instruments and are range measuring devices. This geometric distortion becomes more apparent at steeper incidence angles (typically from 0 to 30 degrees).

The C-HH imagery shows that the agricultural fields exhibit large variations in radar backscatter values. While some fields are characterized by a very low radar return, others display rather bright signatures. One possible explanation for these differences may be related to differences in SWE, however, examination of the SWE values does not support this assumption. For instance, some fields having similar SWE values clearly showed different radar returns. An alternative explanation relates to variations in ground cover type and/or roughness. Most of the fields surveyed were bare with varying levels of surface roughness while some had vegetation and other were pasture. It would appear, therefore, that the ground surface is an important contributor to the total radar backscatter. This hypothesis was further supported by field observations showing that the snowpack was dry at the time the SAR imagery was taken, thereby allowing transmission of the microwave energy through the pack.

Generally speaking, forests appear brighter than do agricultural fields. Volumetric scattering within the forest canopy is the major contributor to the total radar backscatter. The signature of agricultural fields is a combination of scattering within the snowpack, surface scattering from the soil surface, and multiple scattering at and between the soil/snow interface and the snowpack.

Figure 3: SAR C-HH line 4 image of Woodstock site: 13/12/89

The city of Woodstock can be clearly identified on the radar image. The particular geometry of houses and buildings (orthogonal planes) results in the generation of high backscatter values. Smooth streets act as specular reflectors of the microwave energy, hence their dark signature. In addition, the St. John River was not completely frozen, and large ice floes are visible on the imagery.

Field D-1, where an ARC and a corner reflector were deployed during the SAR overpasses, is shown in Figure 3. A total of 5 recirculation points were generated by the ARC, while the corner reflector is seen as a single point on the imagery. Figure 4 displays an enlarged portion of the C-HH imagery, showing field D-1 and surrounding fields. The CR and the ARC are now clearly visible.

February 90 data:

The C-band HH nadir mode image is shown in Figure 5. The horizontal "banding" in the imagery is caused by an unequal distribution of the microwave energy in the across track direction. The image is similar to that obtained in December 89, with forested areas appearing as bright targets, and agricultural fields appearing as darker tones. Although similar in appearance to December, the signature of these fields differ in two ways:

1) The appearance of thin bright linear features, especially in the mid to upper portion of the imagery;

2) A noticeable reduction in contrast between some of the fields.

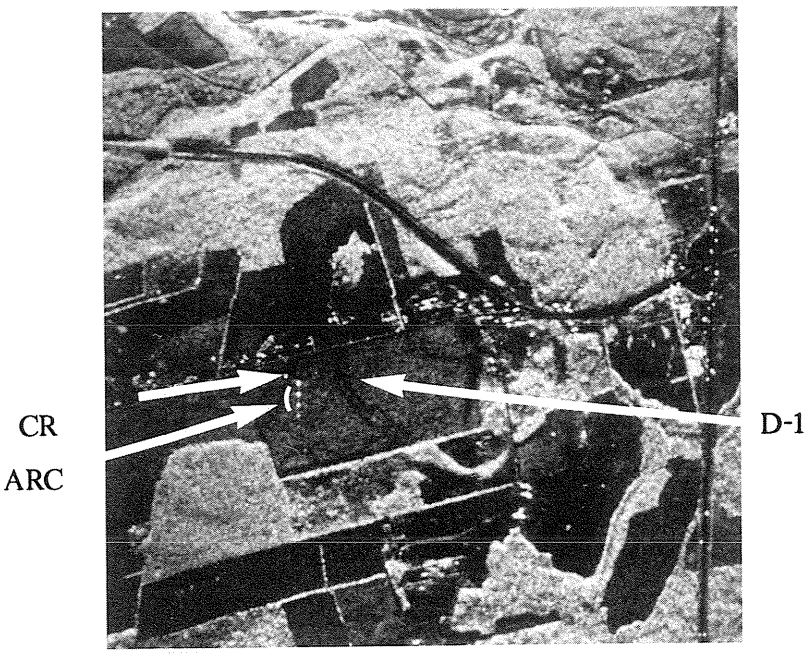

Figure 4: ARC and CR at site D-1

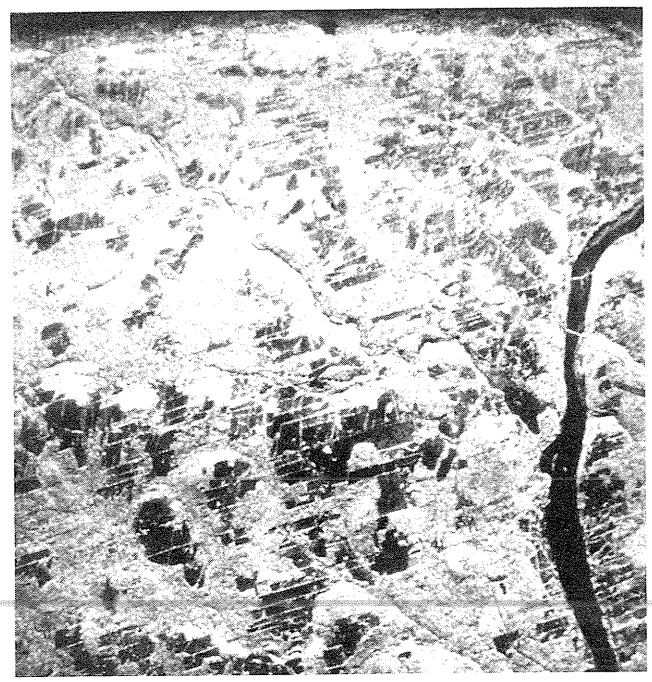

Figure 5: SAR C-HH line 4 image of Woodstock site: 06/02/90

The presence of the bright linear features running across some of the fields does not lend itself to an obvious explanation. Examination of Figure 5 reveals that most of these fields are located in the upper portion of the imagery, i.e. at steep incidence angles. This suggests that these features may be incidence angle dependent. The configuration of the features may also suggest that they are related to drainage patterns within the snowpack or at the soil surface. The observed presence of an unfrozen soil surface in some of the fields reinforces the latter hypothesis. When saturated, the unfrozen soil may generate high backscatter values. However, these drainage patterns should then run along the main slope of the fields.

Further examination reveals that all of these features are oriented along an approximate north-south axis. Consequently, another possible mechanism would be related to snow drifting which results in an uneven snowpack surface. The presence of "waves" at the surface of the pack is not an uncommon occurrence. Westerly winds would generate waves oriented in a north-south direction. Following a rainfall episode, an ice layer forming at the top of the pack would preserve the ondulating pattern. The existence of such a layer, 3 to 5 cm thick, was confirmed by field measurements. Its occurrence may be responsible for the observed linear features. It should be noted that the fields which exhibit these linear features are located in areas which are very exposed to winds, whereas other fields located approximately at the same range from the radar, but which are more sheltered, do not exhibit these patterns (see Figure 5).

Assuming that the soil surface did not change between the two SAR missions, the differences in backscatter values should be related in some complex fashion to variations of the snow cover properties. The apparent reduction in contrast between agricultural fields may be the result of an increase in the SWE. Using a simple backscatter model developed by Ulaby et al. (1982), Leconte and Pultz (1990) have proposed that the total backscatter from a snow covered surface will increase with an increase in SWE for smooth fields, whereas a decrease in the total radar return should occur in rough fields. The model does not account for any multiple scattering effects which may occur between layers in a snowpack, and therefore should be used with caution in analyzing the February data. Nevertheless, observations from this simple model seem to support the hypothesis that increasing the SWE decrease the dynamic range of the observed radar signatures. Another explanation for this apparent reduced contrast may be related to the presence of liquid water in the pack. However, ground measurements indicated that the pack was dry, and that dielectric values did not differ from that of dry snow. There is a need to further investigate these hypotheses through a rigorous digital analysis of calibrated SAR data, in which topographic, surface roughness, and system related effects will be removed or minimized.

Analysis of the SAR data

It becomes obvious from the SAR imagery shown above that the extraction of SWE from SAR data is not a straightforward task, as the contribution to the total backscatter from the soil surface cannot be neglected and, in many situations (longer wavelengths, thin snow packs), it dominates the signal.

Two modelling approaches will be utilized for the quantitative analysis of the SAR data. The first approach, known as the "change detection technique", consists in relating temporal changes in radar returns to changes in snow coverage. Ulaby, et al. (1982) have indicated that this approach may be quite useful in estimating SWE over large areas. Roth, et al. (1985) also noted that improved capabilities for snow mapping are expected through multidate observations.

In addition to the change detection technique, which is entirely empirical, a semi-empirical approach, based on the "cloud model" developed by Ulaby, et al. (1982), will be tested. The model as the following form:

$$\sigma^{\circ}(\theta) = \gamma^{2}(\theta) * \frac{\sigma_{v} \cos\theta'}{2k_{e}} * 1 - \frac{1}{L^{2}(\theta')} + \frac{\sigma_{s}^{\circ}(\theta')}{L^{2}(\theta')} \qquad (1)$$

where

$\gamma(\theta)$	=	power transmission coefficient of the snow-air boundary, dimensionless
θ	=	angle of incidence from nadir
σ_v	=	volume reflectivity of snow, 1/cm
k_e	=	volume extinction coefficient of snow, 1/cm
	=	k_a+k_s, the absorption and scattering coefficients, respectively
θ'	=	angle of refraction, related to θ by Snell's law
$\sigma_s^\circ(\theta')$	=	backscattering coefficient of the underlying ground medium
$L(\theta')$	=	loss factor of the snow layer
$L(\theta')$	=	$\exp(k_e\ d\ \sec\ \theta')$, where d is the snow depth in cm.

This approach ignores diffuse scattering (which accounts for multiple scatter in the snowpack) and multiple reflections between the air-snow and the snow-soil interfaces within which the snow layer is bounded.

Shi, et al. (1990) have proposed an interesting approach for SWE estimation based on equation (1), which employs ratios and differences of HH and VV polarization images. This approach, or a variation of it, will be tested in this study. Carver (1987) has also suggested an approach based on the cloud model, which employs a combination of three frequencies. However, because only C- and X-band data are available, this approach will not be considered.

An essential requirement to both the change detection technique and the cloud model approach to SWE estimation is for calibrated imagery. For example, the change detection approach requires the SAR data to be relatively calibrated, so that any change in reflectances caused by system instabilities be removed, leaving only changes resulting from variations in SWE. Calibration algorithms are under development at CCRS, and softwares will be available in a near future.

In addition to the calibration of the SAR data, other preprocessing tasks will be performed in preparation for the SWE analysis. These are:

- geometric corrections of the imagery (for example to remove the range compression characterizing nadir mode images);
- radiometric corrections (for example to remove the antenna pattern);
- filtering of the data to reduce the "speckle", a salt and pepper texture inherent to any SAR images;
- registration of the imagery to a common base map.

The proposed analyses will make full use of the capabilities of digital image analysis systems and will be carried out in a GIS environment. Field boundaries and the gamma ray coverages will be digitized and attributes, such as slope, aspect, snow depth, SWE, roughness, will be entered in a data base for optimal use by the GIS. Average radar backscatter values will be extracted for each field and gamma ray coverages and imported into the GIS data base, allowing to investigate any relationships between the radar signal and SWE.

CONCLUSION

The very preliminary results obtained so far suggest that SAR data may be suitable for the extraction of SWE values over open areas. However, several issues will need to be addressed. Among them:

- the effect of soil surface properties (roughness, vegetation) on SWE estimation from SAR data;
- the effect of topography on the ability to extract SWE from SAR data;
- the effect of snowpack stratification, grain size and shape, and other structural features on the backscatter properties of the snowpack;
- the possibilities and limitations of SAR for SWE estimation in forested environments.

It is evident here that a simple qualitative analysis of airborne SAR data will not be sufficient for extraction SWE, and that sophisticated image analysis techniques will be required.

In addition, the translation from airborne to satellite data will complicate the issue because of the coarser resolution of these systems. Nevertheless, satellites such as RADARSAT, will have certain advantages over airborne systems: less costly repetitive coverage; larger areas of coverage; smaller incidence angle variations across a swath; and since these systems will be electronically more stable, use of external calibration (using ARCs and CRs) may not be necessary.

The 1990's will bring forth the launch of several satellites carrying onboard SAR payloads. The all weather capability of these systems warrants an assessment of their suitability for the extraction of snow cover information for hydrological applications. This study is a step in that direction.

REFERENCES

Bernier, P.Y. (1987). "Microwave remote sensing of snowpack properties: potential and limitations". Nordic Hydrology, Vol. 18, pp. 1-20.

Bernier M., and J.P. Fortin (1989). "Suivi de la couverture de neige au moyen d'un radar a ouverture synthetique". Proceedings of the IGARSS'89 12th Canadian Symposium on Remote Sensing, Vol. 3, pp 1251-1255.

Brunfeldt, D. (1987). "Theory and design of a field portable dielectric measurement system". Proceedings of IGARSS'87 Symposium, Ann Arbor, 18-21 May 1987, pp 559-563.

Carroll, S.S. and Carroll, T.R. (1990). "Simulation of airborne snow water equivalent measurement errors in extreme environments". Nordic Hydrology (in press)

Carroll, S.S. and Carroll, T.R. (1989A). "Effect of uneven snow cover on airborne snow water equivalent estimates obtained by measuring terrestrial gamma radiation". Water Resources Research. 25 (7), pp 1505-1510.

Carroll, S.S. and Carroll, T.R. (1989B). "Effect of forest biomass on airborne snow water equivalent estimates obtained by measuring terrestrial gamma radiation". Remote Sensing of Environment. 27 (3), pp 313-319.

Carver, K. (1987). "Synthetic Aperture Radar". Earth Observing System Instrument Panel Report, Vol. IIf, NASA, 233 pages.

Chang, A.T.C., J.L. Foster, and D.K. Hall. (1987). "Nimbus-7 SMMR derived global snow cover parameters". Annals of Glaciology 9, 7 pages.

Colbeck, S. (1978). "The difficulties of measuring the water saturation and porosity of snow". Journal of Glaciology, Vol. 20, pp. 189-201.

Glynn, J.E., Carroll, T.R., Holman, P.B., and Grasty, R.L. (1988). "An airborne gamma ray snow survey of a forest covered area with deep snowpack". Remote Sensing of Environment. Vol. 26, No. 2, pp. 149-160.

Goodison, B.E. (1989). "Determination of areal snow water equivalent on the Canadian Prairies using passive microwave satellite data". Proceedings of IGARSS'89 12th Canadian Symposium on Remote Sensing, 10-14 July 1989, Vol. 3, pp 1243-1246.

Goodison, B.E., S.E. Waterman, E.J. Langham (1980). "Application of syntheric aperture radar data to snow cover monitoring". Proceedings of the 6th Canadian Remote Sensing Symposium, Halifax, N.S., May 21-23 1980, pp. 263-271.

Goodison, B.E. 1978. "Accuracy of snow samples for measuring shallow snow packs: an update". Proceedings 35th Annual Meeting Eastern Snow Conference, pp. 36-49.

Hallikainen, M., and F.T Ulaby (1986). "Dielectric and scattering behaviour of snow at microwave frequencies". Proceedings of IGARSS'86 Symposium, Zurich, 8-11 Sept 1986, pp. 87-91.

Hobbs, P.V. (1974). "Ice physics". Clarendon Press, Oxford, U.K. 837 pages.

Jones, E.B. (1983). "Snowpack ground truth manual". NASA contract NAS 5-26802, 42 pages.

Leconte, R. and T.J. Pultz (1990). "Utilisation of SAR dta in the monitoring of snowpacks and wetlands". Proceedings of the Workshop on Application of Remote Sensing in Hydrology, Saskatoon, Sask., February 13-14, 1990.

Livingstone, C.E. et al. (1988). "CCRS C/X airborne synthetic aperture radar: an R and D tool for the ERS-1 time frame. Proceedings of IEEE Nat. Radar Conf. Ann Arbor, Mi. April 20-21.

Matzler, C., and E. Schanda (1984). "Snow mapping with active microwave sensors". International Journal of Remote Sensing, Vol. 5, No. 2, pp. 409-422.

Rango, A., et al. (1990). "Average areal water equivalent of snow in a mountain basin using microwave and visible satellite data". IEEE Transactions on Geoscience and Remote Sensing, Vol. 27, No. 6, pp 740-745.

Rott, H., G. Domik, C. Matzler, H. Miller, K.G. Lenhart (1985). "Study on use and characteristics of SAR for land snow and ice applications". Final report, ESA contract No. 5441/83/D/IM(SC), 117 pages.

Schanda, E. (1987). "On the contribution of volume scattering to the microwave backscattered signal from wet snow and wet soil". International Journal of Remote Sensing, Vo. 8, No. 10, pp. 1489-1500.

Shi, J., J. Dozier, and R.E. Davis. (1990). "Simulation of snow-depth estimation from multi-frequency radar". Proceedings of the IGARSS'90, Washington, D.C., pp. 1129-1132.

Stiles, W.H., and F.T. Ulaby (1980). "Microwave remote snesing of snowpacks". NASA contractor report 3263, Contract NAS5-23777, 404 pages.

Ulaby, F.T., R.K. Moore, A.K. Fung (1982). "Microwave remote sensing - active and passive". Vol II, Addison-Wesley Publishing Company.